Rh 4*d* spin polarization of valence states in Co-Rh

J.-J. Gallet, J.-M. Mariot, L. Journel, and C. F. Hague*
Laboratoire de Chimie Physique–Matière et Rayonnement (URA 176), Université Pierre et Marie Curie, 11 rue Pierre et Marie Curie, 75231 Paris Cedex 05, France

J.-P. Kappler* and G. Schmerber
Institut de Physique et Chimie des Matériaux de Strasbourg (UMR 46), Groupe d'Etude des Matériaux Métalliques, 23 rue du Loess, 69037 Strasbourg Cedex, France

D. J. Singh
Naval Research Laboratory, Washington, D.C. 20375-5320

G. Krill
Laboratoire pour l'Utilisation du Rayonnement Electromagnétique (CNRS–CEA–MENSR), Campus Universitaire d'Orsay, 91405 Orsay Cedex, France

J. Goulon and A. Rogalev
European Synchrotron Radiation Facility, B.P. 220, 38043 Grenoble Cedex, France
(Received 28 July 1997)

X-ray fluorescence spectra involving Rh valence states in Co-Rh-based alloys have been recorded using circularly polarized photons from the Helios II helical undulator at ESRF. Magnetic circular dichroism in the x-ray emission (XEMCD) is observed. To help identify the significance of the XEMCD signal, spin-polarized density functional electronic structure calculations for Co_3Rh have been performed using the general potential linearized augmented plane wave method and appropriate transition matrix elements included to calculate spin-polarized spectra. The theoretical spin polarization is in excellent agreement with experiment inso far as both reveal that, at rhodium sites, polarization is concentrated close to the Fermi edge. The width of the peak in spin polarization can be varied by substituting Ru or Pd for Rh. The size of the change is discussed in relation to the measured magnetization and interpreted with the help of a generalized Slater-Pauling approach [A. R. Williams *et al.*, IEEE Trans. Magn. **MAG-19**, 1983 (1983)]. [S0163-1829(98)07713-3]

I. INTRODUCTION

Coincident with growing interest in magnetic multilayer devices, magnetic circular dichroism in x-ray absorption (XMCD) has developed into a major tool for studying magnetic materials. XMCD provides information on spin and orbital moments via complex sum rules involving the relative intensities of electron excitations from spin-orbit split core levels into empty conduction states.[1] Compared to photoelectron techniques, x-ray absorption has the advantage of larger sampling depths, hence its ability to measure such multilayer devices. XMCD is also used to examine alloys, though, in this case, their magnetic properties are better understood through accumulated macroscopic measurements pursued over many years (see, for instance, Ref. 2). One of the largely outstanding issues is the effect of hybridization on the spin polarization of valence states taken site by site in an alloy (for a review see Ref. 3). This was treated theoretically in the 1970s and 1980s as band structure calculations with spin polarization became tractable, but direct experimental backing was missing because of the difficulty of combining the resolution in spin and element selectivity. Certainly photoelectron experiments were able to measure the spin-resolved valence densities of states (DOS) or, to be more precise, the electron distribution curves,[4] but contributions from each element could only be distinguished in split-band systems. Lately, spin-resolved x-ray photoelectron spectroscopy has been developed[5] with some success but site selectivity is still not provided directly.

Here we report on magnetic circular dichroism in x-ray emission (XEMCD) which measures the spin polarization of valence states with site selectivity. The principle of the method is straightforward. When circularly polarized photons are employed to excite spin-orbit split core levels in magnetically oriented samples, the probability of creating an up-spin or down-spin core hole is different according to whether the incident photon angular momentum is parallel or antiparallel to the magnetization of the sample. As suggested by Strange *et al.*[6] and demonstrated experimentally by Hague *et al.*,[7] the spin imbalance in the core-hole state may be used as a direct probe of the valence spin polarization via the radiative transition of an up-spin or down-spin electron from the valence band (assuming that there is no spin flip).

Two major difficulties are encountered as compared to XMCD experiments. First, the secondary x rays are emitted as a spherical wave so that only a fraction of the signal can be captured by the x-ray analyzer and, second, fluorescence yield is generally low. This means that the highest possible incident flux must be used. Such experiments are a typical justification for third-generation synchrotron radiation

sources. Other problems which have to be faced such as multielectron excitations including Coster-Kronig transitions have been discussed elsewhere.[8–10]

In XEMCD only photons are involved: Photons are incident and photons are measured, which means that experiments are impervious to the presence of even strong magnetic fields. This is the strongest motivation for developing the technique.

We have chosen to investigate the Rh $4d$ spin-polarized DOS in Co-Rh alloys. $4d$ elements are normally paramagnetic but should exhibit a magnetic moment induced by an increase in volume to a critical value (see, for instance, Ref. 11) or by a neighboring ferromagnetic transition metal. The latter may be formed in an alloy or a multilayer structure, with a $3d$ ferromagnetic element.

At present, full-potential relativistic spin-polarized band structure calculations are routinely applied to alloys.[3] We chose bulk alloys for these first XEMCD measurements involving a $4d$ element and a confrontation with theoretical spectra based on first principles calculations.

II. EXPERIMENT

Experiments were performed at the ID12A beam line at ESRF. The first harmonic of the Helios II helical undulator[12] was used to excite the spectra without further monochromatization. This meant that the incident flux was of the order of 10^{15} photons s^{-1} within a bandpass of approximately 140 eV at 3100 eV. Higher harmonics were efficiently cut off by use of mirrors. The latter also reduced the heat load on the samples to a few watts. Approximately $10\times 10\ mm^2$ samples were bonded to a liquid-nitrogen-cooled copper support. The angle of incidence of the photons measured relative to the sample surface was 20° and the take-off angle was normal to the surface to keep self-absorption effects low while still intercepting the full width of the undulator peak ($\approx$1.5 mm) and accommodating the small fluctuations in beam position. The analyzing spectrometer was of the Johann type using a quartz $(10\bar{1}1)$ crystal bent to a radius of 0.7 m. The spectrometer is of a novel design: The sample (and therefore source) is on the Rowland circle as is the position-sensitive detector.[13] The resolution was estimated to be 1.5 eV by measuring the Ag $L\alpha_{1,2}$ lines at 2.98 keV.[14]

High-purity materials were used to produce argon-melted, splat-cooled, annealed (at 900 °C for 72 h), and polished samples. These were fully characterized as concerns magnetization and structure. The investigation hinged on $Co_{75}Rh_{25}$. This bulk alloy was hexagonal close packed (hcp ϵ phase). A number of ternary alloys were also explored by substituting Ni for Co or a $4d$ element (Pd or Ru) for Rh. $(Ni_{15}Co_{85})_{75}Rh_{25}$, $Co_{75}(Rh_{85}Pd_{15})_{25}$, and $Co_{75}(Rh_{75}Pd_{25})_{25}$ were face centered cubic (fcc α phase) with small traces of the ϵ phase due to slight inhomogeneities in the melt. $Co_{75}(Rh_{85}Ru_{15})_{25}$ persisted in the ϵ phase.

Figure 1 shows the shape of the magnetization curves at room temperature for the five alloys studied. During the x-ray emission measurements, the samples were magnetized in a constant field $H\approx 0.25$ T provided by a permanent Nd-Fe-B magnet.[15] XEMCD was obtained by recording spectra with the undulator alternately set to the + or − phase (plus or minus helicity, respectively). The degree of circular polarization had been measured previously to be 97%.[16] A different set of data was also taken with the magnetic field reversed. This operation was performed manually by reversing the position of the permanent magnet. Each set of data was obtained for a rigorously defined geometry. Differences between XEMCD signals from the two sets of data were insignificant.

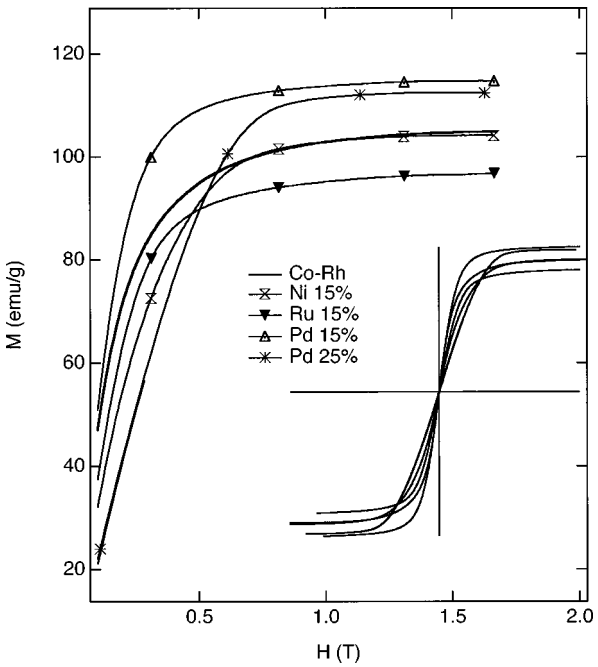

FIG. 1. Magnetization curves at room temperature for $Co_{75}Rh_{25}$, $(Co_{85}Ni_{15})_{75}Rh_{25}$, $Co_{75}(Rh_{85}Ru_{15})_{25}$, $Co_{75}(Rh_{85}Pd_{15})_{25}$, and $Co_{75}(Rh_{75}Pd_{25})_{25}$ shown on an expanded scale for clarity (solid curves are shown as an inset).

III. RESULTS

Figure 2 presents the Rh $L\beta_{2,15}$ x-ray emission for parallel and antiparallel alignments of the photon angular momentum and the magnetic field. The upper panel indicates the difference in the two signals. At this point, we should mention that the original prediction for XEMCD (Ref. 6) proposed the use of resonant excitation [excitation into empty conduction states just above the Fermi energy (E_F) rather than towards the continuum] to enhance the magnitude of the dichroism, yet the first experiments used polychromatic radiation.[7] As we argued at the time, this was a considerable simplification experimentally and it was later demonstrated that deconvolution of the XEMCD signal into separate contributions from occupied and unoccupied conduction states was not so straightforward.[8–10] On the other hand, using polychromatic excitation may introduce artifacts due to multielectron excitations and diffuse scattering. In the present experiments a good compromise is attained because excitation is well to continuum states well above L_3, yet the energy of the incoming photons falls short of the L_2 ionization threshold [the full width at half maximum (FWHM) of the bandpass and the Rh $L_{2,3}$ spin-orbit splitting is $\approx$140 eV]. Even though the energy is sufficient to create shake-up excitations,[10] most of the satellite structure is eliminated as we have shown elsewhere.[17] The L_1-$L_2N_{4,5}$ Coster-Kronig channel is closed because the undulator peak energy distri-

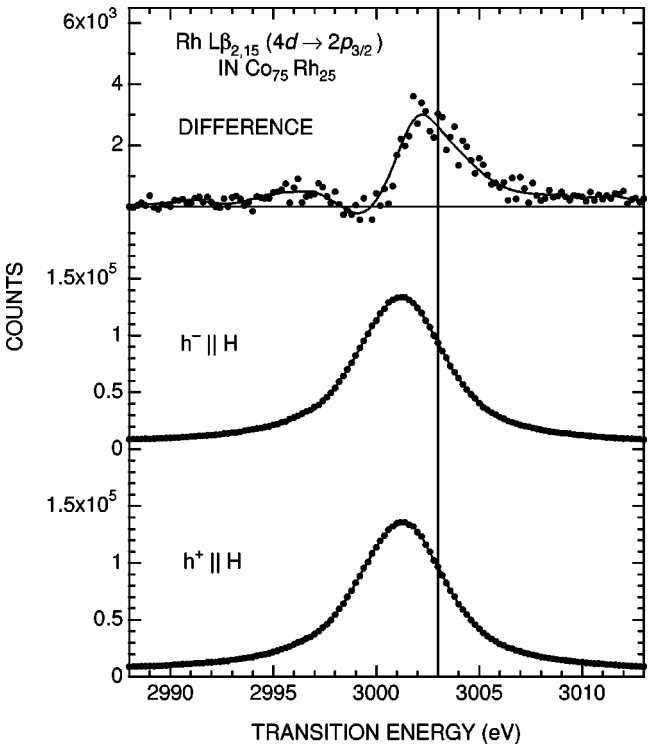

FIG. 2. Rh $L\beta_{2,15}$ x-ray fluorescence spectra obtained with helicity of incoming photons set parallel to magnetic field H and antiparallel to H. Top panel shows difference between the two spectra. Raw data are shown.

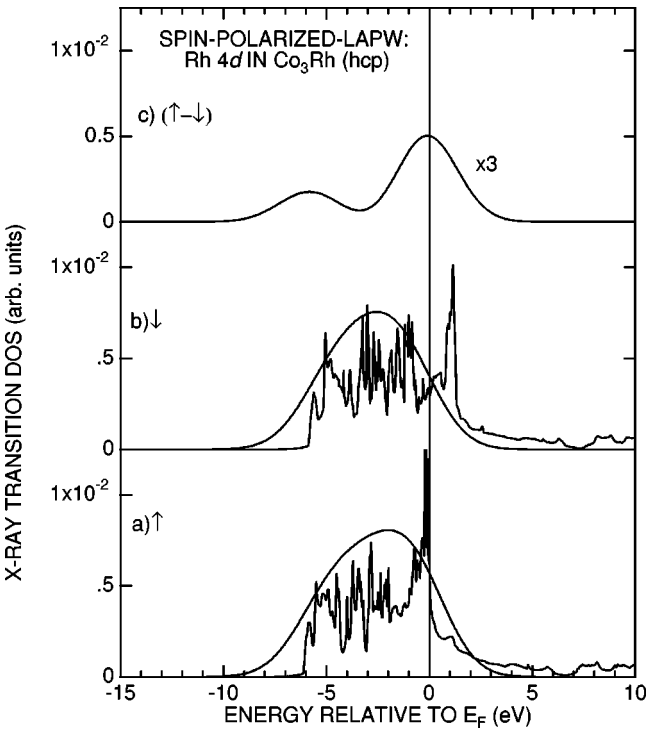

FIG. 3. Spin-polarized relativistic LAPW calculations of the partial local Rh 4d transition densities of states for Co_3Rh in the hcp phase. The difference between majority and minority spins is shown in the top panel. Also shown is the density of states convoluted with a Gaussian curve to simulate experimental broadening.

bution cuts off well before L_1. Moreover, integrating over the appropriate energy limits in the undulator peak distribution shows that contributions from the L_2-L_3N_{45} Coster-Kronig channel may be neglected. A further correction to dichroism in x-ray fluorescence which should be considered[10,18] is the effect of polarization-dependent Auger decay rates. Here we are dealing with L_3-N_{45} radiative transitions, while the dominant Auger processes are L_3-MM, and so here again corrections are negligible. Possible diffuse scattering is eliminated for photon energies below the L_3 threshold, though a contribution to dichroism above the L_3 edge cannot be ruled out.

The shape of the XEMCD signal shown in the upper panel of Fig. 2 is unexpected insofar as it is very different from that previously observed for the Co L_3 emission.[19,20] We will come back to this point later.

Although we are dealing with a disordered alloy, we may reasonably compare our spectra with linearized augmented plane wave (LAPW) calculations for the ordered hcp Co_3Rh intermetallic compound. The different sizes of Co and Rh ions were expected to lead to substantial relaxations, which could affect the spectra significantly, as well as providing a driving force for local ordering. The present full-potential LAPW calculations[21] were done with well-converged basis sets and Brillouin zone samplings using the experimental hexagonal lattice parameters. Co and Rh layers were stacked in an hcp fashion using an assumed ordering . . . RhCoCoCoRhCoCoCoRh . . . . Total energy calculations showed a substantial relaxation of the layer spacings, so that the Co-Rh interlayer distance became 2.17 Å and the Co-Co layer spacing was 1.99 Å. Core states were treated fully relativistically, while valence states were treated in a scalar relativistic approximation. The calculated spin magnetization of $1.39\mu_B$ per atom corresponds to $1.86\mu_B$ per Co atom, somewhat larger than the magnetization of hcp Co ($1.72\mu_B$), reflecting polarization of the Rh which has a moment of $0.6\mu_B$. The spectra were calculated by weighting the DOS by the relevant core-valence dipole matrix elements. These were calculated from the full LAPW wave functions. Roughly described, the Co 3d DOS (not shown) has a bandwidth of $\approx$3.4 eV (majority and minority spin bands have the same width) and a spin polarization which is similar to that of pure Co (see Ref. 22). This is well understood in terms of the Stoner criterion:[23] In a strong ferromagnet spin-down electrons flip into spin-up states until they are full. The energy of the system is further lowered by the fact that E_F then lies in a dip in the minority spin DOS.

In ϵ-Co_3Rh there are two inequivalent Co sites but differences in the corresponding partial DOS are negligible. The Rh transition DOS for the alloy are presented Fig. 3. There is only one type of Rh site in the ordered phase. Fortunately for the ensuing discussions the DOS for paramagnetic fcc rhodium have the same overall shape as in the hcp alloy. The Rh minority spin band is a little narrower than that of the majority states but the main difference is the appearance of a sharp peak in the occupied majority states close to E_F. At E_F the majority DOS is approximately twice that of the minority states, rising to 3 times the minority states 0.15 eV below E_F.

The outcome (as seen in the top panel of Fig. 3) is that the spin polarization is dominated by a strong dichroic signal just below E_F, followed by a dip 4 eV below E_F and again

followed by a rise in the relative DOS of the majority states at the bottom of the band. The difference curve is very similar to that observed experimentally after convolution with a Gaussian function representing instrumental broadening. It is clear, however, that the agreement concerning the shapes of the calculated and observed emission spectra is poor. When a Lorentzian broadening function is added to represent core-hole lifetime the calculated emission is broader still and the general agreement with experiment is not improved. It should be remembered that the two x-ray emission spectra contain different contributions from up and down spins, and so are not directly related to the up and down DOS. The FWHM observed is 4.3 eV as opposed to 6 eV according to the LAPW calculations. This is despite the inclusion of the x-ray transition matrix elements in the calculation. As a matter of fact this is a classic observation for transition-metal x-ray emission spectra[24,25] or even photoemission valence band data[26,27] and is mainly the result of relaxation effects in the intermediate state. This has been illustrated theoretically very recently for resonant x-ray fluorescence for graphite.[28] There are pronounced differences between the x-ray emission calculated within the one-particle approximation and when relaxation is taken into account.

A quantitative comparison between experiment and theory for the XEMCD signal reveals the following situation. The calculated asymmetry defined as $[(n^{\uparrow}-n^{\downarrow})/(n^{\uparrow}+n^{\uparrow})]$ is 8.5%. The experimental asymmetry is therefore expected to be one-quarter of that (2.13%) taking into account the relative probabilities for creating spin-up or spin-down core holes.[29] The experimental value is 0.75%. The correction for the degree of circular polarization (97%) and for the angle between the angular moment of the incoming photons and the direction of magnetization is small. This leaves us with a value of the order of 1%. (Here 1% may even be an overestimate because, as pointed out above, the high-energy tail to the dichroic signal may originate in shake-up satellites:[10] Because of the broad bandpass of the incoming photons, we were not able to elucidate this point.) The most likely explanation is that magnetic saturation was not attained during measurements (see Fig. 1) despite liquid nitrogen cooling. So far, therefore, we conclude that agreement between experiment and theory is only qualitative.

According to the magnetization curves (Fig. 1), saturated magnetization is higher if Pd is substituted but decreases if Ru is substituted. It is unchanged for $(Co_{85}Ni_{15})_{75}Rh_{25}$. In the latter case and especially that of $Co_{75}(Rh_{75}Pd_{25})_{25}$, a higher field is required to attain saturation. The corresponding XEMCD data are given in Fig. 4. The FWHM of the XEMCD peak in $Co_{75}Rh_{25}$, $(Co_{85}Ni_{15})_{75}Rh_{25}$, and $Co_{75}(Rh_{75}Pd_{25})_{25}$ is $\approx$2.4 eV; it is broader (2.7 eV) in $Co_{75}(Rh_{85}Pd_{15})_{25}$, but distinctly narrower (1.9 eV) in $Co_{75}(Rh_{85}Ru_{15})_{25}$.

IV. DISCUSSION

Crangle and Parsons[2] measured the total magnetic moments of a number of 3*d*-4*d* and 3*d*-5*d* alloys (see Fig. 5). They found that the magnetic moment of Co-4*d* alloys drops rapidly as Ru is added, drops less rapidly as Rh is added, and still less rapidly as Pd is added (a 10% drop in μ_B occurs for 4%, 6%, and 15% additions of the respective 4*d* elements).

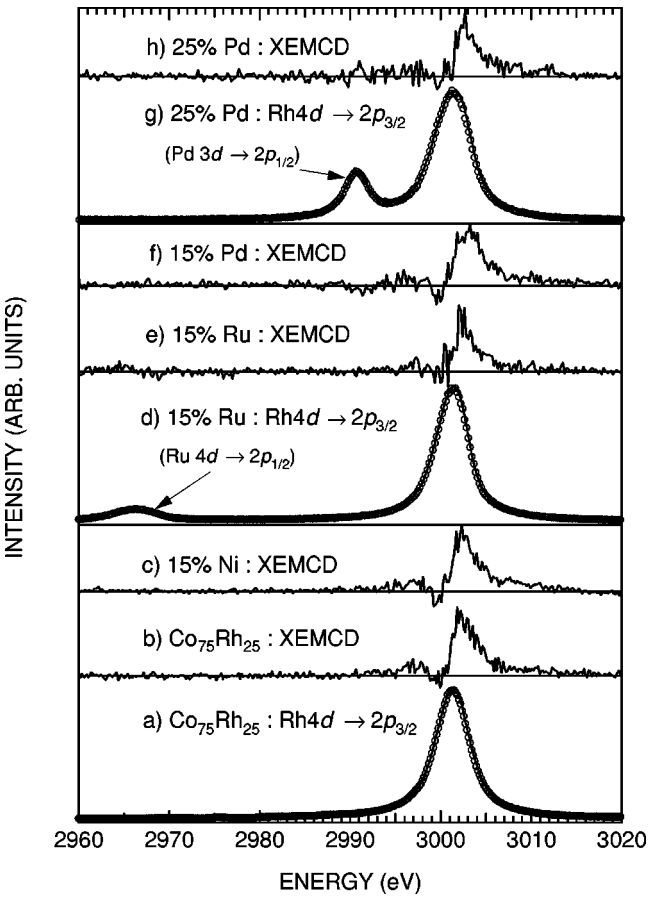

FIG. 4. Rh $L\beta_{2,15}$ x-ray fluorescence spectra for three of the Co-Rh alloys studied with helicity of incoming photons set parallel to magnetic field H (solid line) and antiparallel to H (open circles). The XEMCD (raw data) is shown for all five alloys.

They were amongst the first to conclude that the magnetic moment was not an average value over all atoms. They proposed that only Pd possessed a significant moment, the moment for Rh being zero and that for Ru being negative. From these remarks we could crudely conclude that adding Pd or Ru should indeed affect the magnetization curve as in Fig. 1; i.e., substituting Pd for Rh should lead to a higher average moment per atom with the opposite effect for Ru. Along the same lines, and still referring to the measurements for binary alloys in Ref. 4, substituting Ni for Co should dramatically reduce the average moment and saturation magnetization because moments for Ni-rich Rh alloys are less than half the values found for the Co alloys. This is not observed. Moreover, it has been shown experimentally by means of XMCD that the moment at Rh sites is in fact $\approx 0.62\mu_B$ in a coevaporated $Co_{77}Rh_{23}$ film.[30] Such films are fcc with cellular disorder and the corresponding XMCD spectra calculated from density functional theory using the Korringa-Kohn-Rostoker coherent potential approximation are in agreement with experiments.[31]

To interpret the data it is tempting to apply simple reasoning based on rigid shifts in the paramagnetic states as electrons are transferred from spin-down to spin-up states. Indeed there is little alternative short of performing complex calculations on ternary cellularly disordered alloys. The most instructive model is the generalized Slater-Pauling construction proposed by Williams *et al.*[32,33] It is empirical in its

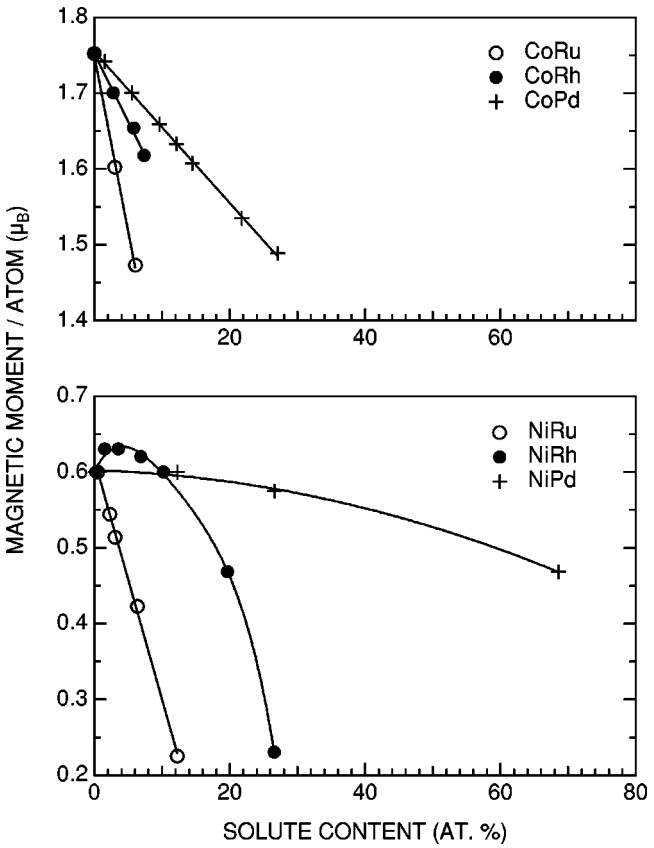

FIG. 5. Magnetic moments of Co and Ni alloys. The curves are adapted from measurements by Crangle and Parsons (see Ref. 2).

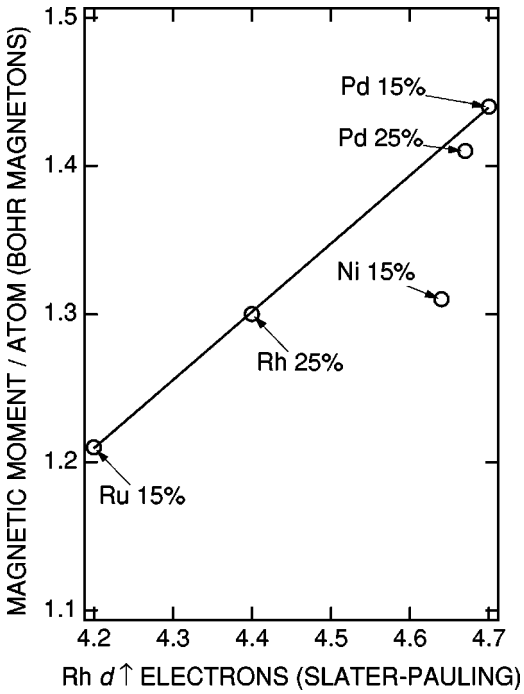

FIG. 6. Magnetic moments per atom deduced from Fig. 1, plotted against the Rh majority spin count deduced using a generalized Slater-Pauling construction (see Refs. 31 and 32).

approach, yet is founded on a good understanding of the spin-resolved DOS and has proved its reliability in explaining trends in magnetic properties, both in split-band and common-band regimes. Williams *et al.* define a key parameter termed the magnetic valence Z_m. We follow their formulation in rewriting the magnetic moment per atom, $\mu=n^{\uparrow}-n^{\downarrow}$, as $\mu=2(n_{sp}^{\uparrow}+n_d^{\uparrow})-Z$, where Z is the total number of valence electrons; $Z_m=2n_d^{\uparrow}-Z$. It is explicitly assumed that $n_{sp}^{\uparrow}$ remains constant as long as only transition metals are involved; i.e., alloying two transition metals is unlikely to strongly modify the more dispersive sp bands. $n_d^{\uparrow}$ for Co, a strong ferromagnet, corresponds to five electrons, and so $Z_m=1$, $n_{sp}^{\uparrow}\approx 0.3$ electrons. The average valence for a binary alloy $A_{1-x}B_x$ is $Z_{\mathrm{av}}=(1-x)Z_A+xZ_B$. Z_{av} is constant for Co-Rh, and so the expression for μ tells us trivially that if the average magnetic moment for the alloy, μ_{av}, decreases, $n_d^{\uparrow}$ decreases also. From our magnetization measurements $\mu_{\mathrm{av}}=1.3$ which is compatible with the value extrapolated from the measurements by Crangle and Parsons (Fig. 5). Thus from the expression $\mu_{\mathrm{av}}=2(0.3+0.75n_{d\,\mathrm{Co}}^{\uparrow}+0.25n_{d\,\mathrm{Rh}}^{\uparrow})-Z_{\mathrm{av}}$, we find that $n_{d\,\mathrm{Rh}}^{\uparrow}=4.4$ electrons.

If we now substitute Pd for Rh, Z_{av} goes from 9 in Co-Rh to 9.04 in $\mathrm{Co}_{75}(\mathrm{Rh}_{85}\mathrm{Pd}_{15})_{25}$ and we deduce from Fig. 1 that μ_{av} increases to $1.44\mu_B$. It means that $(n_d^{\uparrow})_{\mathrm{av}}$ must increase both to compensate for the increased value of μ_{av} and Z_m. In Pd the majority spin band is full, and so an increase in $n_d^{\uparrow}$ must come from Rh sites: $n_{d\,\mathrm{Rh}}^{\uparrow}$ increases to ≈ 4.7 electrons. The spin-up–spin-down imbalance has almost doubled compared to $\mathrm{Co}_{75}\mathrm{Rh}_{25}$. It explains the larger Rh XEMCD. On the contrary Z_{av} drops to 8.97 for $\mathrm{Co}_{75}(\mathrm{Rh}_{85}\mathrm{Ru}_{15})_{25}$, and μ_{av} to $1.21\mu_B$. Ruthenium like iron at best would be a weak magnet. Thus the drop in $n_d^{\uparrow}$ is expected again to affect the Rh sites most. This time $n_{d\,\mathrm{Rh}}^{\uparrow}=4.2$ electrons. The XEMCD signal confirms this trend.

$Z_{\mathrm{av}}=9.11$ for $(\mathrm{Co}_{85}\mathrm{Ni}_{15})_{75}\mathrm{Rh}_{25}$. This is the largest value amongst this set of alloys. In a Co-Ni alloy μ_{av} decreases regularly as Ni is added.[34] This is clearly compatible with the fact that we are dealing with two strong ferromagnets, i.e., $n_d^{\uparrow}=5$ electrons for both Co and Ni; $(n_d^{\uparrow})_{\mathrm{av}}$ does not change but Z_{av} increases. It is surprising, therefore, that we do not observe a decrease in either μ_{av} for this ternary alloy or the Rh XEMCD compared to $\mathrm{Co}_{75}\mathrm{Rh}_{25}$. $n_{d\,\mathrm{Rh}}^{\uparrow}$ should increase from 4.4 to 4.6 electrons, but this is not reflected in our XEMCD experiment. This discrepancy is brought out by plotting the magnetic moment per atom deduced from Fig. 2 against $n_{d\,\mathrm{Rh}}^{\uparrow}$ deduced in the way described (Fig. 6). It may be attributed to hybridization between Ni and Rh in the vicinity of E_F. We have already emphasized that the Co $3d$ majority spin states are very depleted at E_F, which is not the case for Ni. From Fig. 5 we see that the average magnetic moment increases in $\mathrm{Ni}_{100-x}\mathrm{Rh}_x$ compared to pure Ni in the region of small x, no doubt for the same reason. Whereas Co and Rh are practically in the split-band regime, Ni and Rh as far as the DOS close to E_F are concerned form a common band.

Now we have to explain why the Rh XEMCD signal for $\mathrm{Co}_{75}(\mathrm{Rh}_{75}\mathrm{Pd}_{25})_{25}$ is smaller than for $\mathrm{Co}_{75}(\mathrm{Rh}_{85}\mathrm{Pd}_{15})_{25}$. Despite the need for a higher field to attain saturation in the former, magnetization saturation has the same value in both alloys. Z_{av} has increased only from 9.04 to 9.06 but Pd contributes five $n_d^{\uparrow}$ electrons, and so $n_{d\,\mathrm{Rh}}^{\uparrow}$ must be reduced to

compensate. The magnetic valence of Rh drops back to its value in $Co_{75}Rh_{25}$.

V. CONCLUSION

The generalized Slater-Pauling construction put forward by Williams *et al.*, already tested against a wide range of magnetic alloys, successfully explains how the size of the Rh XEMCD depends on the addition of Ru and Pd in these alloys. According to this model changes should be observed when Ni is substituted for Co, but this is not case. We propose that this is due to the fact that, at least as concerns DOS just below E_F, hybridization partially changes from a split-band (Co-Rh) to a common-band (Ni-Rh) regime. The coherence between the magnetization measurements and the XEMCD strengthens the hypothesis that the x-ray fluorescence spectra are not only spin selective but also relate to valence state spin polarization.

Saturated magnetization was not specifically sought for in these experiments, and so quantitative conclusions concerning the magnetic properties of these alloys are not expected. Nevertheless, we conclude that the width of the Rh XEMCD relates the spin-up and spin-down cutoff at E_F. The two bands are indeed essentially shifting rigidly with respect to each other. The size of the shift is very small (enough to accommodate ± 0.3 electrons) but with a tendency to stabilize at 4.3 spin-up electrons in the valence band.

The balance between the spin polarization at Rh sites and the average magnetic valence is quite subtle, and so self-evident interpretations cannot be made. These experiments have been performed on relatively strong magnetic materials. The challenge now lies with the study of more weakly magnetized alloys or nominally nonmagnetic materials in which moments are induced by the proximity of a ferromagnetic element.

ACKNOWLEDGMENT

We wish to thank the Centre National de la Recherche Scientifique for financial support.

*Also at Laboratoire pour l'Utilisation du Rayonnement Electromagnétique (CNRS–CEA–MENSR), Campus Universitaire d'Orsay, 91405 Orsay Cedex, France.

[1] B. T. Thole, P. Carra, F. Sette, and G. van der Laan, Phys. Rev. Lett. **67**, 3590 (1991).
[2] J. Crangle and D. Parsons, Proc. R. Soc. London, Ser. A **255**, 509 (1960).
[3] J. B. Staunton, Rep. Prog. Phys. **57**, 1289 (1994).
[4] E. Kisker, in *Metallic Magnetism*, edited by H. Capellmann, Topics in Current Physics, Vol. 42 (Springer, Berlin, 1986), p. 57.
[5] L. E. Klebanoff, D. G. Van Campen, and R. J. Pouliot, Rev. Sci. Instrum. **64**, 2863 (1993).
[6] P. Strange, P. J. Durham, and B. L. Gyorffy, Phys. Rev. Lett. **67**, 3590 (1991).
[7] C. F. Hague, J.-M. Mariot, P. Strange, P. J. Durham, and B. L. Gyorffy, Phys. Rev. B **48**, 3560 (1993).
[8] L.-C. Duda, J. Stöhr, D. C. Mancini, A. Nilsson, N. Wassdahl, J. Nordgren, and M. G. Samant, Phys. Rev. B **50**, 16 758 (1994).
[9] C. F. Hague, J.-M. Mariot, G. Y. Guo, K. Hricovini, and G. Krill, Phys. Rev. B **51**, 1370 (1995).
[10] S. Eisebitt, J. Lüning, J.-E. Rubensson, D. Schmitz, S. Blügel, and W. Eberhardt, Solid State Commun. **104**, 173 (1997).
[11] V. L. Moruzzi and P. M. Marcus, Phys. Rev. B **39**, 471 (1989).
[12] P. Elleaume, J. Synchrotron Radiat. **1**, 19 (1994).
[13] C. F. Hague, P. Avila, and D. Laporte (unpublished).
[14] C. F. Hague, J.-M. Mariot, and H. Ostrowiecki, Phys. Lett. **67A**, 121 (1978).
[15] C. F. Hague, J.-J. Gallet, and J.-M. Mariot, Appl. Phys. A: Mater. Sci. Process **65**, 141 (1997).
[16] L. Varga, C. Giles, C. Neumann, A. Rogalev, C. Malgrange, J. Goulon, and F. de Bergevin, J. Phys. IV **7**, C2-309 (1997).
[17] J.-J. Gallet, J.-M. Mariot, C. F. Hague, J.-P. Kappler, J. Goulon, A. Rogalev, G. Krill, M. Sacchi, and K. Hricovini, J. Phys. IV **7**, C2-365 (1997).
[18] L. Braicovich, C. Dallera, G. Ghiringelli, N. B. Brookes, and J. B. Goedkoop, Phys. Rev. B **55**, 14 729 (1997).
[19] J.-M. Mariot and C. F. Hague, J. Phys. IV **4**, C9-453 (1994); C. F. Hague and J.-M. Mariot, Nucl. Instrum. Methods Phys. Res. B **97**, 449 (1994).
[20] L.-C. Duda, Ph.D. thesis, Uppsala University, 1996.
[21] D. J. Singh, *Planewaves, Pseudopotentials and the LAPW Method* (Kluwer, Boston, 1994).
[22] D. A. Papaconstantopoulos, *Handbook of the Band Structure of Elemental Solids* (Plenum, New York, 1986).
[23] O. Gunnarsson, J. Phys. F **6**, 587 (1976).
[24] P. J. Durham, D. Ghaleb, B. L. Gyorffy, C. F. Hague, J.-M. Mariot, G. M. Stocks, and W. M. Temmerman, J. Phys. F **9**, 1719 (1979).
[25] P. J. Durham, C. F. Hague, J.-M. Mariot, and W. M. Temmerman, J. Phys. (Paris), Colloq. **48**, C9-1059 (1987).
[26] F. J. Himpsel, J. A. Knapp, and D. E. Eastman, Phys. Rev. B **19**, 2919 (1979).
[27] W. Eberhardt and E. W. Plummer, Phys. Rev. B **21**, 3245 (1980).
[28] M. van Veenendaal and P. Carra, Phys. Rev. Lett. **78**, 2839 (1997).
[29] Ruqian Wu, Dingsheng Wang, and A. J. Freeman, in *Magnetic Ultrathin Films*, edited by B. T. Jonker *et al.*, MRS Symposia Proceedings No. 313 (Materials Research Society, Pittsburgh, 1993), p. 541.
[30] G. R. Harp, S. S. P. Parkin, W. L. O'Brien, and B. P. Tonner, Phys. Rev. B **51**, 12 037 (1995).
[31] H. Ebert, J. Phys. IV **7**, C2-161 (1997).
[32] A. R. Williams, V. L. Moruzzi, A. P. Malozemoff, and K. Terakura, IEEE Trans. Magn. **MAG-19**, 1983 (1983).
[33] A. R. Williams, A. P. Malozemoff, V. L. Moruzzi, and M. Matsui, J. Appl. Phys. **55**, 2353 (1984).
[34] *Zahlenwerte und Funktionen*, Landolt-Börnstein, Auflage 6, Band II, Teil 9 (Springer, Berlin, 1962).